

## Resonant Raman Scattering by Phonons in a Strong Magnetic Field: GaAs

G. Ambrazevičius,<sup>(a)</sup> M. Cardona, and R. Merlin<sup>(b)</sup>

*Max-Planck-Institut für Festkörperforschung, D-7000 Stuttgart 80, Federal Republic of Germany*

(Received 27 May 1987)

We have measured Raman scattering by LO phonons in GaAs in a magnetic field ( $\leq 12.8$  T) at 10 K. The intensity displays Landau-level oscillations. This effect shows promise as a modulation technique for the investigation of interband magnetoabsorption. As an application we have studied the nonparabolicity of the  $\Gamma_1$  conduction band of GaAs for energies up to 0.4 eV above its bottom. Standard  $\mathbf{k} \cdot \mathbf{p}$  expansions, including the  $\Gamma_1$  and  $\Gamma_{15}$  conduction and the  $\Gamma_{15}$  valence bands, cannot explain the observed dispersion. It can be explained by inclusion of interactions with higher bands.

PACS numbers: 71.25.Tn, 78.20.Ls, 78.30.Fs

Resonant Raman scattering by phonons near the lowest direct edge of zinc-blende-type semiconductors ( $E_0$ ) has been profusely studied in the past twenty years.<sup>1</sup> These studies include GaAs<sup>2,3</sup> and GaAs-based superlattices.<sup>4,5</sup> Here we investigate this phenomenon for GaAs in the presence of a magnetic field. Strong oscillations are seen which correspond to interband transitions between Landau subbands, a fact which emphasizes the modulation-spectroscopy aspects of resonant Raman scattering.<sup>6</sup> We can follow these transitions to energies higher than in any previous experiments.<sup>7,8</sup> This fact enables us to perform a precise study of the nonparabolicity of the  $\Gamma_1$  conduction band. The observed peaks cannot be fitted with a five-band  $\mathbf{k} \cdot \mathbf{p}$  model. However, this deficiency can be easily corrected by the introduction of a diagonal term in the Hamiltonian proportional to  $k^2$  which should correspond to the sum of all interactions between  $\Gamma_1$  and remote higher bands. This term is related to the constant  $C \cong -2$  introduced by Hermann and Weisbuch<sup>9</sup> and also in more recent publications.<sup>10-13</sup> By lumping this constant  $C$  together with the interaction with the  $\Gamma_{15}$  conduction band, we obtain a new diagonal constant  $C^*$  which must be made equal to  $-3.2 \pm 0.2$  in order to fit the observed magneto-Raman resonances.

The measurements were performed on high-purity (100) surfaces of GaAs prepared by liquid-phase epitaxy. The samples are  $n$ -type with  $N_e = 7 \times 10^{12} \text{ cm}^{-3}$  and mobility  $\mu \cong 10^5 \text{ cm}^2/\text{V} \cdot \text{s}$  ( $T = 77$  K). As incident light we used several lines of the  $\text{Ar}^+$  and  $\text{Kr}^+$  ion lasers and a DCM (4-dicyanomethylene-2-methyl-6- $p$ -dimethylaminostyryl-4 $H$ -pyran) dye laser (Coherent Radiation Inc. model No. 590) pumped with a cw  $\text{Ar}^+$  laser. A SPEX Industries Inc. double monochromator was set at a fixed frequency corresponding to the light scattered by the LO phonon (Stokes shift of  $294 \text{ cm}^{-1}$ ) for each incident laser line. The slits were kept wide open, with a spectral slit width of  $9 \text{ cm}^{-1}$ . The detector was an RCA photomultiplier model No. C31034A with photon counting electronics. The maximum field provided by our split-coil superconducting magnet (Intermagnetics, mod-

el No. SO-9068) is 12.8 T. For each laser frequency the scattered intensity was measured in the Faraday configuration with  $\mathbf{B}$  along the [001] crystal direction and  $\hat{\mathbf{e}}_L, \hat{\mathbf{e}}_S$  (incident and scattered polarizations) parallel to [100] and also with  $\hat{\mathbf{e}}_L \parallel [100]$  and  $\hat{\mathbf{e}}_S \parallel [010]$ . Measurements with circularly polarized light are planned for the future.

Typical data are shown in Fig. 1 for the laser photon energy  $\hbar\omega_L = 1.769$  eV. The values of  $n$ , the Landau quantum number of the conduction electrons associated with each maximum, were determined as discussed below. We note that integer values of  $n$  usually correspond to maxima although  $n = 18$  has been assigned to a minimum. The Landau oscillations of Fig. 1 are superimposed on a rising background. This effect is possibly related to the magnetic-field-enhanced scattering by LO modes reported by Gammon, Merlin, and Morkoç<sup>14</sup> for superlattices. Whether an integer value of  $n$  corresponds

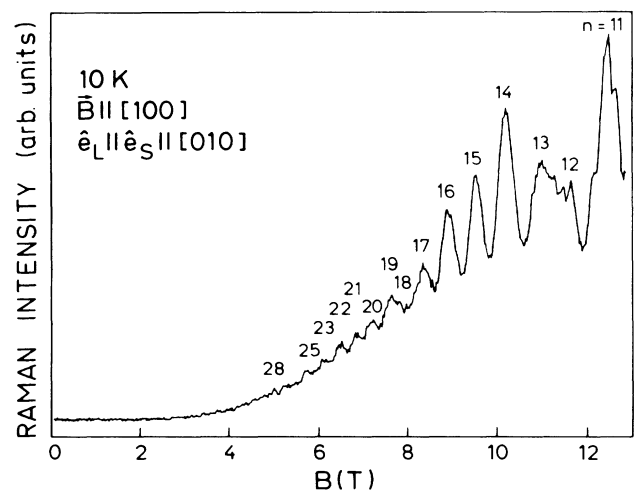


FIG. 1. Magneto-Raman resonances for scattering by LO phonons in GaAs with the magnetic field in Faraday configuration. The  $n$ 's indicate the Landau quantum number of the corresponding conduction subband.

to a maximum or minimum of the oscillations depends on the phase of the resonant part of the Raman susceptibility relative to the background. A detailed study of these interference effects, which requires the separation of the Raman susceptibility into Fröhlich and deformation-potential contributions,<sup>1</sup> will be published at a later date.

The maxima observed for eight different laser frequen-

cies are plotted in Fig. 2 versus magnetic field. We have also plotted in this figure (solid lines) the energies of the transitions between the heavy-hole Landau subbands and the conduction bands for the same value of  $n$  (note, however, that the selection rules require<sup>15</sup> either  $\Delta n=0$  or  $\Delta n=2$ ; separation of these two cases should be possible with circular polarizations). The energies of these transitions were calculated with the expression<sup>16</sup>

$$\hbar\omega_L - E_0 = -\frac{E_0^*}{2} + \left[ \left( \frac{E_0^*}{2} \right)^2 + E_0^* \left( \frac{m_0}{m_{e0}^*} - 1 - C^* \right) \frac{\hbar e B}{m_0 c} \left( n + \frac{1}{2} \right) \right]^{1/2} + \frac{\hbar e B}{m_0 c} \left( \frac{m_0}{m_{hh}^*} + 1 + C^* \right) \left( n + \frac{1}{2} \right), \quad (1)$$

where the gap  $E_0 = 1.520$  eV,  $E_0^* = E_0 + \Delta_0/3 = 1.631$  eV,  $m_0$  is the free-electron mass,  $m_{e0}^*$  the effective mass of the electrons at the bottom of the  $\Gamma_1$  band,  $C^*$  a dimensionless constant to be discussed below, and  $m_{hh}^*$  the nearly  $n$ -independent mass of the heavy holes. We took for the plot of Fig. 2  $m_{e0}^* = 0.0665m_0$  and  $m_{hh}^* = 0.48m_0$  (from *Landolt-Börnstein Tables*<sup>17</sup>) and also  $C^* = -3.2$  as representing the best fit to the experimental data.

It is apparent in Fig. 2 that the theoretical lines explain most of the observed peaks. Those which do not fall on one of the lines usually fall halfway between them, a fact which suggests that in this case the frequencies of Eq. (1) correspond to a resonance minimum. In a few cases, especially at high fields (see peaks 11-13 in

Fig. 1), the peaks split into several components most of which can be identified as related to  $\Delta n=2$ . One should also keep in mind that structures in the Raman susceptibility are also expected if we replace  $\omega_L$  by the scattered frequency  $\omega_S$  in Eq. (1) [outgoing resonances; those of Eq. (1) are incoming resonances]. The outgoing resonances should be out of phase with the incoming ones and one of the latter for a given  $n$  should occur close to one of the former with a 2 to 4 units smaller  $n$ . Thus, beatings between incoming and outgoing resonances may result. They are probably responsible for the weakness

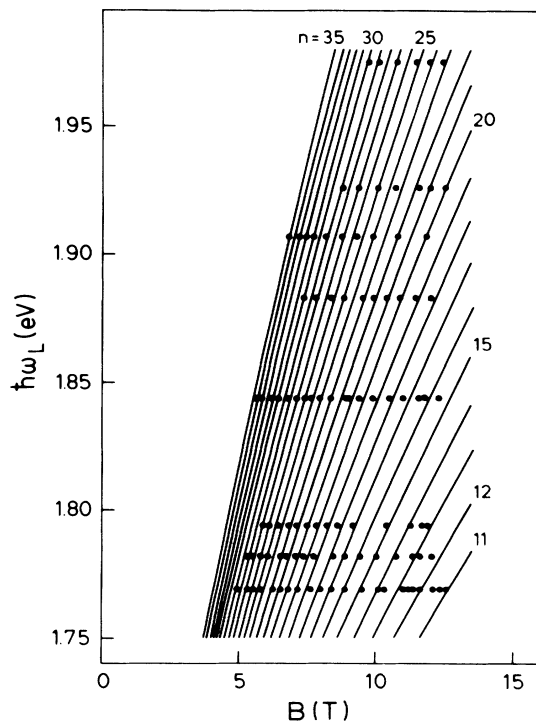


FIG. 2. Position of the maxima observed in spectra such as that of Fig. 1. The lines were calculated with Eq. (1) for  $C^* = -3.2$ .

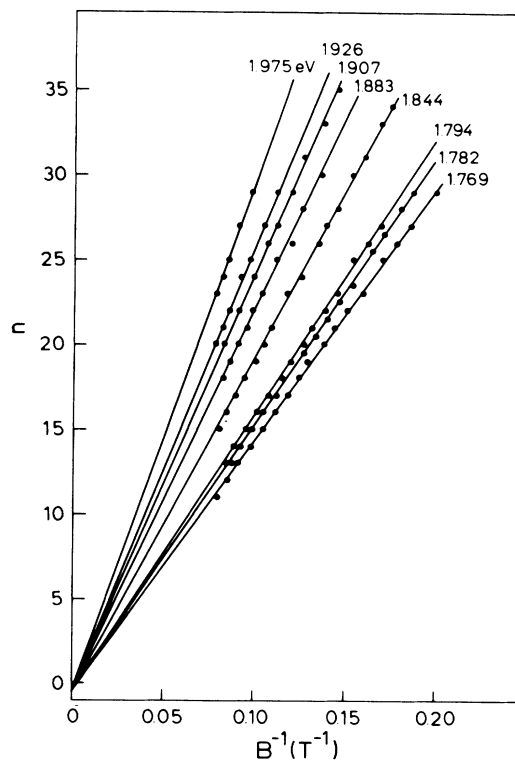


FIG. 3. Landau number of experimental peaks as determined from Fig. 2 plotted vs  $B^{-1}$  for the eight experimental laser frequencies. The lines were calculated with Eq. (1) for  $C^* = -3.2$ .

of the structures 18, 12, and 13 in Fig. 1. A detailed study of these effects is on the way.

Figure 3 displays the values of  $B^{-1}$  ( $x$  axis) vs  $n$  ( $y$  axis) as calculated with Eq. (1) for eight values of  $\hbar\omega_L$  used in our experiments. It follows from Eq. (1) that these plots must be linear and converge to  $n = -\frac{1}{2}$  for  $B \rightarrow \infty$ . The experimental points plotted in Fig. 3 fall on the calculated lines for integer values of  $n$ , with the exception of a few which had to be assigned to half-integer  $n$ 's as already pointed out above. In order to obtain the good correspondence between the experimental points

$$\hbar\omega_L - E_0 = E_F + (\hbar^2 k^2 / 2m_0)(m_0/m_{hh}^*),$$

$$E_F = -\frac{E_0^*}{2} + \left[ \left( \frac{E_0^*}{2} \right)^2 + E_0^* \left( \frac{m_0}{m_{e0}^*} - 1 - C^* \right) \frac{\hbar^2 k^2}{2m_0} \right]^{1/2} + \frac{\hbar^2 k^2}{2m_0} (1 + C^*). \quad (2)$$

The effective mass  $m_e^* = m_e^*(E_F)$  was obtained with the equation

$$\frac{1}{m_e^*} = \frac{c}{eB} \frac{d\omega_L}{dn} = \frac{1}{\hbar^2 k} \frac{dE_F}{dk}, \quad (3)$$

with use of Eq. (1) for the dependence of  $\hbar\omega_L$  on  $n$ . Two such plots are given, one for  $C^* = -3.2$  (the value of Figs. 2 and 3) and the other for  $C^* = 0$ . The plot for  $C^* = -3.2$  can be considered as an experimental determination of  $m_e^*$  for the eight values of  $E_F$  corresponding to the  $\hbar\omega_L$ 's used in our measurements (see vertical arrows in Fig. 4 and also Fig. 3). Deviations can be seen for values of  $C^*$  which differ from  $-3.2$  by more than  $\pm 0.2$ . Hence we take this to be the error bars of our experimental determination ( $C^* = -3.2 \pm 0.2$ ). The dashed line in Fig. 4, obtained for  $C^* = 0$ , shows a nonparabolic increase in  $m_e^*$  which is nearly half that found in the present work. We have also included in Fig. 4 several other experimental values (points) of  $m_e^*$  obtained in doped materials for different  $E_F$ 's.<sup>18</sup> They scatter around the solid line calculated for  $C^* = -3.2$  and deviate considerably from that for  $C^* = 0$ .

It is not *a priori* obvious that the effect of  $C^*$  on the Landau levels can be treated as in Eq. (1). Actually  $C^*$  must be first included as a diagonal term in  $k^2$  in the  $4 \times 4$  Hamiltonian for  $B=0$  [Eq. (2)] and then the effect of the magnetic field must be treated by our solving eight coupled differential equations. It is easy to show, however, that  $C^*$  can be included as in Eq. (1) for large values of the Landau quantum number  $n$ .  $C^*$  contains a contribution from the lowest  $\Gamma_{15}$  conduction bands, which is often treated separately,<sup>9-11,13</sup> plus another, labeled  $C$ , from all other bands. The  $\Gamma_{15}$  contribution has been estimated to be equal to  $-1.9$ ,<sup>9-12</sup> and  $-1$ .<sup>10,11,13</sup> Estimates for the  $C$  contribution are  $-2$ ,<sup>9,10,12,13</sup> and  $-1.9$ .<sup>11</sup> This leads to values of  $C^*$  between  $-3$  and  $-4$  which are in agreement with our result.

We note that a nonparabolicity above that predicted

and the calculations it is necessary to take  $C^* = -3.2 \pm 0.2$  in Eq. (1). We note that similar values of  $C^*$  are required to explain the peaks observed with piezoreflectance in Ref. 8 for  $n > 6$  (no detailed calculations were given in Ref. 8 for GaAs, probably because of this difficulty).

The need to include  $C^*$  in Eq. (1) in order to explain our data, especially those for large  $\hbar\omega_L$  is best illustrated in Fig. 4 where we have plotted  $m_e^*$  versus the energy above the bottom of the conduction band  $E_F$  found by simultaneously solving the equations

by the standard  $\mathbf{k} \cdot \mathbf{p}$  two- or four-band model has been also observed for the  $L_1$  conduction band of germanium in magneto-piezotransmission experiments near the *indirect* edge.<sup>19</sup> The observed effect can be explained by the introduction of a constant  $C^* = -2.6$ , rather similar to the one discussed here.

In GaAs there is a second direct gap labeled  $E_0 + \Delta_0$  at 1.86 eV (4 K). Magneto-optical oscillations associated with this edge have been observed in piezoreflectance experiments.<sup>20</sup> They have not been seen in our work, a fortunate fact which enables us to observe the  $E_0$  oscillations to higher frequencies than in previous works. The failure to see  $E_0 + \Delta_0$  can be explained by the absence of diagonal matrix elements of the deformation potential at

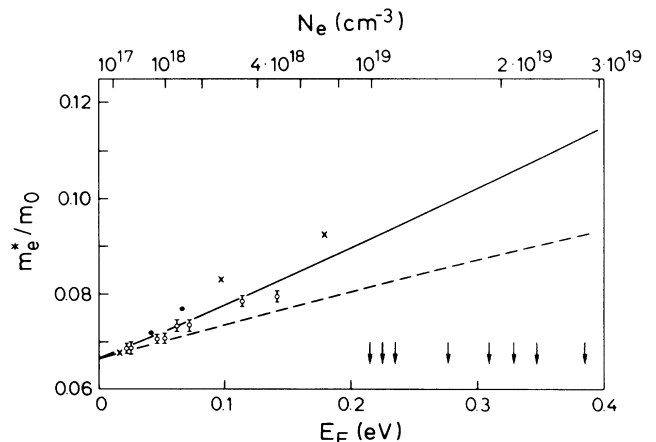


FIG. 4. The solid line depicts the electron mass obtained with Eq. (1) for  $C^* = -3.2$  vs energy  $E_F$  above the bottom of the conduction band. Because of the excellent fit in Fig. 3 this curve represents experimental values at the eight  $E_F$ 's given by the vertical arrows. The dashed curve was obtained with Eq. (1) for  $C^* = 0$ . The data points correspond to other determinations of  $m_e^*$  from Ref. 18.

the  $E_0 + \Delta_0$  gap.<sup>1</sup> For the Fröhlich coupling the explanation can be sought in the fact that the scattering efficiency is proportional to<sup>1</sup>

$$[1/m_e^* - 1/m_h^*]^2, \quad (4)$$

where  $m_e^* = 0.0665m_0$  ( $E_F = 0$ ) and  $m_h^* = 0.48m_0$  for heavy holes and  $0.15m_0$  for the split-off hole band ( $E_0 + \Delta_0$  gap). Equation (4) gives for the  $E_0$  edge a scattering efficiency 2.5 times larger than for the split-off band.

We would like to thank Liu Ran for help with the measurements, E. Bauser for preparing the sample, H. Hirt, M. Siemers, and P. Wurster for expert technical assistance, and H. Sigg for a critical reading of the manuscript. Two of us (G.A. and R.M.) acknowledge receipt of fellowships from the Alexander von Humboldt Foundation.

<sup>(a)</sup>On leave from Institut of Semiconductor Physics, Lithuanian Academy of Sciences, 232 600 Vilnius, U.S.S.R.

<sup>(b)</sup>On leave from Department of Physics, The University of Michigan, Ann Arbor, MI 48109.

<sup>1</sup>See, for instance, M. Cardona, in *Light Scattering in Solids II*, edited by M. Cardona and G. Güntherodt (Springer, Heidelberg, 1982), p. 19.

<sup>2</sup>R. Trommer and M. Cardona, *Phys. Rev. B* **17**, 1865 (1978).

<sup>3</sup>A. K. Sood, W. Kauschke, J. Menéndez, and M. Cardona, *Phys. Rev. B* **35**, 2886 (1987).

<sup>4</sup>J. E. Zucker, A. Pinczuk, D. S. Chemla, A. Gossard, and

W. Wiegmann, *Phys. Rev. Lett.* **51**, 1293 (1983).

<sup>5</sup>W. Kauschke, A. K. Sood, M. Cardona, and K. Ploog, *Phys. Rev. B* **36**, 1612 (1987).

<sup>6</sup>M. Cardona, *Surf. Sci.* **37**, 100 (1973).

<sup>7</sup>Q. H. F. Vrethen, *J. Phys. Chem. Solids* **29**, 129 (1968).

<sup>8</sup>M. Reine, R. L. Aggarwal, and B. Lax, *Phys. Rev. B* **5**, 3033 (1972).

<sup>9</sup>C. Hermann and C. Weisbuch, *Phys. Rev. B* **15**, 823 (1977).

<sup>10</sup>W. Zawadzki, P. Pfeffer, and H. Sigg, *Solid State Commun.* **53**, 777 (1985).

<sup>11</sup>U. Rössler, *Solid State Commun.* **49**, 943 (1984).

<sup>12</sup>G. Fasol and H. P. Hughes, *Phys. Rev. B* **33**, 2953 (1986).

<sup>13</sup>H. Sigg, J. A. A. J. Perenboom, P. Pfeffer, and W. Zawadzki, *Solid State Commun.* **61**, 685 (1987).

<sup>14</sup>D. Gammon, R. Merlin, and H. Morkoç, *Phys. Rev. B* **35**, 2552 (1987).

<sup>15</sup>L. M. Roth, B. Lax, and S. Zwerdling, *Phys. Rev.* **114**, 90 (1959); E. Burstein, G. S. Picus, R. F. Wallis, and F. Blatt, *Phys. Rev.* **113**, 15 (1959).

<sup>16</sup>W. Zawadzki, in *Narrow Gap Semiconductors and Applications*, edited by W. Zawadzki (Springer, Heidelberg, 1980), p. 85.

<sup>17</sup>*Landolt-Börnstein Tables*, edited by O. Madelung, M. Schulz, and H. Weiss (Springer, Heidelberg, 1980), Vol. 111–117.

<sup>18</sup>A. Raymond, J. L. Robert, and C. Bernard, *J. Phys. C* **12**, 2289 (1979), and references therein.

<sup>19</sup>R. L. Aggarwal, M. D. Zuteck, and B. Lax, *Phys. Rev. Lett.* **19**, 236 (1967); M. Cardona, *Modulation Spectroscopy* (Academic, New York, 1969), p. 319.

<sup>20</sup>M. Reine, R. L. Aggarwal, B. Lax, and C. M. Wolfe, *Phys. Rev. B* **2**, 458 (1970).